

Spontaneous Circulation in Ground-State Spinor Dipolar Bose-Einstein Condensates

Yuki Kawaguchi,¹ Hiroki Saito,² and Masahito Ueda^{1,3}

¹*Department of Physics, Tokyo Institute of Technology, 2-12-1 Ookayama, Meguro-ku, Tokyo 152-8551, Japan*

²*The University of Electro-Communications, 1-5-1, Choufugaoka, Choufu-shi, Tokyo 182-8585, Japan*

³*Macroscopic Quantum Control Project, ERATO, JST, Bunkyo-ku, Tokyo 113-8656, Japan*

(Received 12 June 2006; published 28 September 2006)

We report on a study of the spin-1 ferromagnetic Bose-Einstein condensate with magnetic dipole-dipole interactions. By solving the nonlocal Gross-Pitaevskii equations for this system, we find three ground-state phases. Moreover, we show that a substantial orbital angular momentum accompanied by chiral symmetry breaking emerges spontaneously in a certain parameter regime. We predict that all these phases can be observed in the spin-1 ⁸⁷Rb condensate by changing the number of atoms or the trap frequency.

DOI: 10.1103/PhysRevLett.97.130404

PACS numbers: 03.75.Kk, 03.75.Lm, 03.75.Mn, 03.75.Nt

The magnetic dipole-dipole interaction in ferromagnets is responsible for a rich variety of spin structures [1]. Similar spin textures can also be expected to occur, due to the dipolar interaction, in ferromagnetic Bose-Einstein condensates (BECs) such as the spin-1 ⁸⁷Rb BEC. However, spinor BECs differ from ferromagnets in that they exhibit spin-gauge symmetry that can generate mass flow by developing spin textures [2]. One may therefore wonder whether the dipole-induced spin texture can yield spontaneous mass current in the ground state. In this Letter we show that this is the case.

An additional motivation for our work is the recent observation of a dipolar BEC in a system of spin-polarized ⁵²Cr atoms [3]. The ground state of spinor dipolar BECs has been studied theoretically by several researchers using a single-mode approximation [4–6]. Magnetism of dipolar BECs in one- and two-dimensional optical lattices has also been investigated [7,8]. In this Letter, we study the ground-state spin textures of a spinor dipolar BEC without invoking the single-mode approximation. We show the existence of three ground-state phases at zero magnetic field. In particular, we identify chiral spin-vortex phase and show that spontaneous circulation with broken chiral symmetry emerges in this phase.

We consider a system of N spin-1 atoms with mass M confined in a spin-independent potential $U_{\text{trap}}(\mathbf{r}) = M\omega^2(x^2 + y^2 + z^2)/2$. The Hamiltonian of the system is given by [9]

$$\begin{aligned} \hat{H}_{\text{tot}} = & \int d\mathbf{r} \left[\hat{\psi}_{m_1}^\dagger(\mathbf{r}) H_0 \hat{\psi}_{m_1}(\mathbf{r}) \right. \\ & + \frac{g_0}{2} \hat{\psi}_{m_1}^\dagger(\mathbf{r}) \hat{\psi}_{m_2}^\dagger(\mathbf{r}) \hat{\psi}_{m_2}(\mathbf{r}) \hat{\psi}_{m_1}(\mathbf{r}) \\ & + \frac{g_1}{2} \hat{\psi}_{m_1}^\dagger(\mathbf{r}) \hat{\psi}_{m_2}^\dagger(\mathbf{r}) \mathbf{F}_{m_1 m_4} \cdot \mathbf{F}_{m_2 m_3} \hat{\psi}_{m_3}(\mathbf{r}) \hat{\psi}_{m_4}(\mathbf{r}) \left. \right] \\ & + \hat{H}_{\text{dd}}, \end{aligned} \quad (1)$$

where $\hat{\psi}_m(\mathbf{r})$ is the annihilation operator of an atom in the magnetic sublevel $m = 0, \pm 1$ at point \mathbf{r} , $H_0 =$

$-\hbar^2 \nabla^2 / (2M) + U_{\text{trap}}(\mathbf{r})$, $\mathbf{F}_{mm'}$ represents the spin-1 matrix, and \hat{H}_{dd} is the contribution of the magnetic dipole-dipole interaction. The spin-independent and spin-dependent interactions are characterized by $g_0 = 4\pi\hbar^2(a_0 + 2a_2)/(3M)$ and $g_1 = 4\pi\hbar^2(a_2 - a_0)/(3M)$, respectively, with a_s ($s = 0, 2$) being the s -wave scattering length for the scattering channel with total spin s . For spin-1 ⁸⁷Rb atoms we have $0 < -g_1 \ll g_0$, and the ground state is ferromagnetic.

The magnetic dipole moment of an atom is given by $\hat{\boldsymbol{\mu}} = -g_S \mu_B \hat{\mathbf{S}} + g_I \mu_N \hat{\mathbf{I}}$, where μ_B is the Bohr magneton, μ_N is the nuclear magneton, $\hat{\mathbf{S}}$ and $\hat{\mathbf{I}}$ are the electronic and nuclear spin angular momenta, respectively, and $g_{S,I}$ are the Landé g factors. The matrix element of the dipole moment between magnetic sublevels in the spin-1 hyperfine manifold is shown to be $\langle m | \hat{\boldsymbol{\mu}} | m' \rangle = g_F \mu_B \mathbf{F}_{mm'}$. For the case of ⁸⁷Rb with $S = 1/2$ and $I = 3/2$, we have $g_F = (g_S + 5g_I \mu_N / \mu_B) / 4 \approx 1/2$. Then the contribution of the magnetic dipole-dipole interaction to the Hamiltonian is given by

$$\begin{aligned} \hat{H}_{\text{dd}} = & \frac{c_{\text{dd}}}{2} \int d\mathbf{r} \int d\mathbf{r}' \hat{\psi}_{m_1}^\dagger(\mathbf{r}) \hat{\psi}_{m_2}^\dagger(\mathbf{r}') \hat{\psi}_{m_3}(\mathbf{r}') \hat{\psi}_{m_4}(\mathbf{r}) \\ & \times \frac{\mathbf{F}_{m_1 m_4} \cdot \mathbf{F}_{m_2 m_3} - 3(\mathbf{F}_{m_1 m_4} \cdot \mathbf{e})(\mathbf{F}_{m_2 m_3} \cdot \mathbf{e})}{|\mathbf{r} - \mathbf{r}'|^3}, \end{aligned} \quad (2)$$

where $c_{\text{dd}} = \mu_0 g_F^2 \mu_B^2 / (4\pi)$ with μ_0 being the magnetic permeability of the vacuum, and $\mathbf{e} = (\mathbf{r} - \mathbf{r}') / |\mathbf{r} - \mathbf{r}'|$. We ignore the coupling of the $F = 1$ manifold with the $F = 2$ manifold due to the dipolar interaction because the hyperfine splitting ~ 100 mK is much larger than the dipolar energy ~ 1 nK.

Our system has three characteristic length scales: dipole healing length $\xi_{\text{dd}} = \hbar / \sqrt{2M c_{\text{dd}} n_0}$, spin healing length $\xi_{\text{sp}} = \hbar / \sqrt{2M |g_1| n_0}$, and Thomas-Fermi (TF) radius $R_{\text{TF}} = 2a_{\text{ho}} [g_0 n_0 / (\hbar\omega)]^{1/2}$, where $n_0 = \hbar\omega / g_0 [5(a_2 + 2a_0)N / (8a_{\text{ho}})]^{2/5}$ is the TF peak density, and $a_{\text{ho}} = [\hbar / (2M\omega)]^{1/2}$. As shown below, the phase diagram is

characterized by two dimensionless parameters $R_{\text{TF}}/\xi_{\text{dd}}$ and $R_{\text{TF}}/\xi_{\text{sp}}$.

We investigate the mean-field ground state of the total Hamiltonian \hat{H}_{tot} . The general form of the ferromagnetic spinor order parameter is given by

$$\begin{pmatrix} \psi_1 \\ \psi_0 \\ \psi_{-1} \end{pmatrix} = \sqrt{n} e^{-i\gamma} \begin{pmatrix} e^{-i\alpha} \cos^2(\beta/2) \\ \sqrt{2} \sin(\beta/2) \cos(\beta/2) \\ e^{i\alpha} \sin^2(\beta/2) \end{pmatrix}, \quad (3)$$

where n is the number density, γ is the gauge, and $\mathbf{s} = (\sin\beta \cos\alpha, \sin\beta \sin\alpha, \cos\beta)$ is the unit vector parallel to the magnetization. The dipolar interaction induces a spin texture characterized by a spatial dependence of Euler angles α, β, γ . This dependence induces mass and spin velocity fields which can be calculated from continuity equations $\partial n/\partial t + \nabla \cdot (n\mathbf{v}) = 0$ and $\partial(n s_\mu)/\partial t + \nabla \cdot (n \mathbf{v}_{\text{sp}}^\mu + n s_\mu \mathbf{v}) = 0$, as $\mathbf{v} = -\hbar/M(\nabla\gamma + \cos\beta\nabla\alpha)$, $\mathbf{v}_{\text{sp}}^z = -\hbar/(2M)\sin^2\beta\nabla\alpha$, and $\mathbf{v}_{\text{sp}}^x + i\mathbf{v}_{\text{sp}}^y = -\hbar/(2M) \times e^{i\alpha}[-\sin\beta \cos\beta\nabla\alpha + i\nabla\beta]$. Here $n\mathbf{v}$ and $n\mathbf{v}_{\text{sp}}^\mu$ ($\mu = x, y, z$) describe the current density of the mass and that of the μ component of the spin vector \mathbf{s} , respectively. In addition to the kinetic energy $K_0 = \int d\mathbf{r} \hbar^2/(2M)|\nabla\sqrt{n}|^2$ arising from the spatial dependence of the total density, the system has kinetic energies $K_{\text{mass}} = \int d\mathbf{r} \frac{1}{2} n M |\mathbf{v}|^2$ and $K_{\text{spin}} = \int d\mathbf{r} n M \sum_\mu |\mathbf{v}_{\text{sp}}^\mu|^2 = \int d\mathbf{r} \hbar^2/(4M) \sum_\mu |\nabla s_\mu|^2$ caused by the mass and spin currents, respectively. In the case of ferromagnets, the domain structure is mainly determined by the interplay between the dipolar interaction and the spin stiffness that has the form of K_{spin} . In the case of dipolar BECs, the additional term K_{mass} is significant.

The ground-state phases can be classified by the symmetry of the order parameter. The total Hamiltonian \hat{H}_{tot} is invariant under space inversion $\mathbf{P}\hat{\psi}_m(\mathbf{r}) = \hat{\psi}_m(-\mathbf{r})$, and time reversal $\mathbf{T}\hat{\psi}_m(\mathbf{r}) = (-1)^m \hat{\psi}_{-m}^\dagger(\mathbf{r})$. It also possesses rotational [i.e., SO(3)] symmetry in combined spin and coordinate space around an arbitrary axis. However, as we show below, the SO(3) symmetry is reduced to uniaxial symmetry, and the obtained phases are eigenstates of the projected total angular momentum $\hat{J}_z = -i(\partial/\partial\varphi) + F_z$ in cylindrical coordinates $\mathbf{r} = (r, \varphi, z)$, characterized by

$$\alpha(\mathbf{r}) = \varphi + \tilde{\alpha}(r, z), \quad (4a)$$

$$\beta(\mathbf{r}) = \beta(r, z) = \beta(r, -z), \quad (4b)$$

$$\gamma(\mathbf{r}) = -J\alpha(\mathbf{r}) + \tilde{\gamma}(r, z), \quad (4c)$$

with J being the eigenvalue of \hat{J}_z . We thus classify the obtained phases by the value of J , space-inversion symmetry, and time-reversal symmetry.

The ground-state phases are obtained by solving the nonlocal Gross-Pitaevskii (GP) equations,

$$(H_0 + g_0 n)\psi_0 + (g_1 f_+ - c_{\text{dd}} b_+) \frac{\psi_1}{\sqrt{2}} + (g_1 f_- - c_{\text{dd}} b_-) \frac{\psi_{-1}}{\sqrt{2}} = \mu \psi_0, \quad (5a)$$

$$(H_0 + g_0 n)\psi_{\pm 1} + (g_1 f_{\mp} - c_{\text{dd}} b_{\mp}) \frac{\psi_0}{\sqrt{2}} \pm (g_1 f_z - c_{\text{dd}} b_z) \psi_{\pm 1} = \mu \psi_{\pm 1}, \quad (5b)$$

where μ is the chemical potential, $n = \sum_m |\psi_m|^2$ is the number density, and $\mathbf{f} = (f_x, f_y, f_z)$ is the spin density defined by $f_z = |\psi_1|^2 - |\psi_{-1}|^2$ and $f_x + if_y = f_+ = f_-^* = \sqrt{2}(\psi_1^* \psi_0 + \psi_0^* \psi_{-1})$. When the system is purely ferromagnetic, the spin density satisfies $\mathbf{f} = n\mathbf{s}$. We define the scaled dipole field $\mathbf{b} = (b_x, b_y, b_z)$ as $b_\mu(\mathbf{r}) = -\sum_{\nu=x,y,z} \int d\mathbf{r}' (\delta_{\mu\nu} - 3e_\mu e_\nu) f_\nu(\mathbf{r}')/|\mathbf{r} - \mathbf{r}'|^3$ and $b_\pm = b_x \pm ib_y$. The effective magnetic field produced by the surrounding magnetic dipoles is given by $c_{\text{dd}} \mathbf{b}/(g_F \mu_B)$.

We numerically solve Eq. (5) in three dimensions by the imaginary-time propagation method. We prepare the initial state by first solving Eq. (5) with $c_{\text{dd}} = 0$, and then randomizing local spin directions, keeping the number density unchanged. Comparing the total energies of the obtained textures, we obtain the phase diagram in the parameter space of $(R_{\text{TF}}/\xi_{\text{sp}}, R_{\text{TF}}/\xi_{\text{dd}})$ as shown in Fig. 1(a). For the spin-1 ^{87}Rb BEC, we have $\xi_{\text{sp}}/\xi_{\text{dd}} = \sqrt{c_{\text{dd}}/|g_1|} = 0.30$, and the system follows the dotted line in Fig. 1(a). A typical spin configuration in each phase is shown in Figs. 1(b)–1(d). The symmetry properties are summarized in Fig. 2. We now describe the properties of each phase.

Polar-core vortex (PCV) phase.—This phase has total angular momentum of $J = 0$ and has a polar core, i.e., $(\psi_1, \psi_0, \psi_{-1}) = \sqrt{n}(0, 1, 0)$ at $r = 0$ [10]. The length of the spin vector $|\mathbf{f}|/n$ is less than unity for $r \lesssim \xi_{\text{sp}}$, and the spin configuration far from the core is described by $\tilde{\alpha} = \pm\pi/2$, $\beta = \pi/2$, and $\tilde{\gamma} = \text{const}$. Since the $m = 1$ component has the phase winding number -1 and the $m = -1$ component has the phase winding number $+1$, the net mass current vanishes while the net spin current remains, giving a non-zero K_{spin} . Time-reversal symmetry and space-inversion symmetry are both broken, but the order parameter remains invariant under the combined PT operation.

Flower (FL) phase [11].—This phase has $J = 1$ and can continuously develop from a spin-polarized state. The spin configuration is given by $\tilde{\alpha}(z > 0) = 0$, $\tilde{\alpha}(z < 0) = \pi$, $0 \leq \beta \ll \pi/2$, and $\tilde{\gamma} = \text{const}$. Since $\beta \sim 0$, most of the total angular momentum $N\hbar$ resides in the spin, and the remaining small angular momentum is carried by mass current. The spin current is also small. The system has space-inversion symmetry while time-reversal symmetry is broken.

Chiral spin-vortex (CSV) phase.—This phase has $J = 1$ and the spin structure is described by $0 \leq \tilde{\alpha} \leq \pi$, $\tilde{\alpha}(r, z) + \tilde{\alpha}(r, -z) = \pi$, and $0 \leq \beta \leq \pi$. The gauge $\tilde{\gamma}$ also varies in space. As shown in Fig. 1(d), this phase

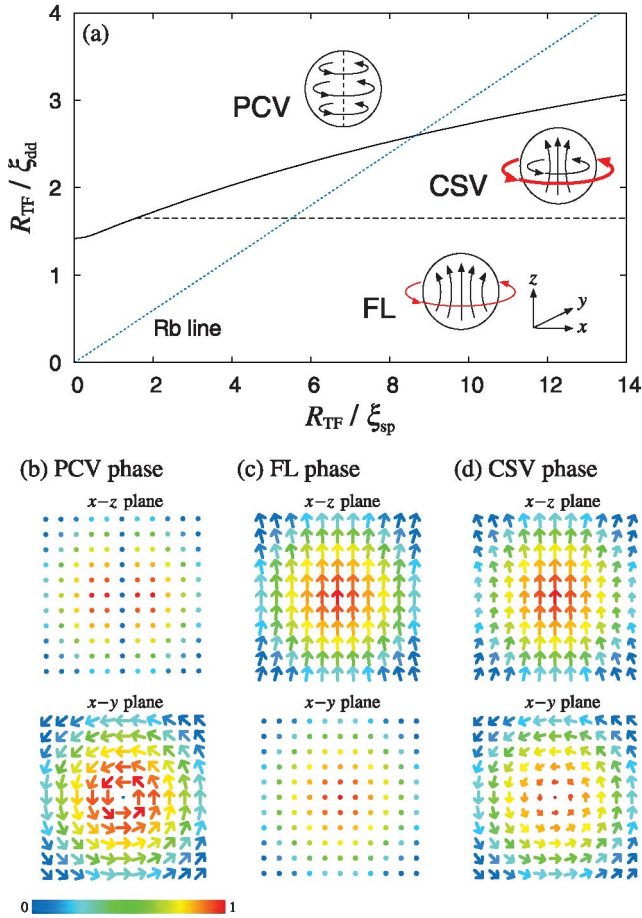


FIG. 1 (color). (a) Phase diagram of a ferromagnetic dipolar BEC. The solid curve shows the first-order phase boundary between the $J = 0$ and $J = 1$ phases, and the broken line represents the second-order one and divides the phases with and without spin chirality, where PCV, CSV, and FL stand for polar-core vortex, chiral spin-vortex, and flower phases, respectively. The schematic shown in each region represents the spin configuration (black arrows) and mass flow (red arrows). The spin-1 ^{87}Rb BEC ($\xi_{sp}/\xi_{dd} = 0.30$) traces the dotted line, which is referred to as the Rb line, as a function of R_{TF}/ξ_{sp} . (b)–(d) Typical spin configuration in each phase. The top and bottom panels show the unit vector $\mathbf{f}(\mathbf{r})/|\mathbf{f}(\mathbf{r})|$ projected onto the $x-z$ and $x-y$ planes, respectively. The color of the arrows represents the magnitude of the spin density normalized by the number density $|\mathbf{f}(\mathbf{r})|/n(\mathbf{r})$ (see the bottom scale).

has a coreless vortex whose size is of the order of ξ_{dd} . The system has substantial spin and mass currents around the rotational axis and has nonzero K_{mass} and K_{spin} . Both time-reversal symmetry and space-inversion symmetry are broken.

The dependence of the dipolar energy on R_{TF}/ξ_{dd} is shown in the inset of Fig. 3. The dipolar energy is minimized when the spin texture has a flux-closure structure [12], i.e., when the divergence of the magnetization is everywhere zero. The PCV state, which satisfies $\nabla \cdot \mathbf{f} = 0$ in all space, has the lowest dipolar energy of the three states.

Phase	J	P	T	PT
PCV $\leftarrow \rightarrow$	0	$\times \leftarrow \rightarrow$	$\times \leftarrow \rightarrow$	$\circ \leftarrow \rightarrow$
FL $\uparrow \uparrow$	1	$\circ \uparrow \uparrow$	$\times \uparrow \uparrow$	$\times \uparrow \uparrow$
CSV $\leftarrow \rightarrow$	1	$\times \leftarrow \rightarrow$	$\times \leftarrow \rightarrow$	$\times \leftarrow \rightarrow$

FIG. 2. Broken (\times) and unbroken (\circ) symmetries for each phase in Fig. 1. The schematic in each cell shows the spin configuration after the transformation by P, T, and PT.

The CSV state is different from the FL state in that the chiral symmetry of the spin vortex is broken to form a flux-closure structure. When the CSV state has a non-zero total angular momentum in the $+\hat{z}$ direction, there are two degenerate whirling patterns of spins in the $x-y$ plane: clockwise ($\tilde{\alpha} < 0$) and anticlockwise ($\tilde{\alpha} > 0$). These patterns have the spin configurations of right-handed and left-handed screws, which are transformed into each other under space-inversion P. The system selects one of the degenerate states by breaking the chiral symmetry. Accompanied by the chiral symmetry breaking, the net orbital angular momentum $L_z = \int d\mathbf{r} \sum_m \psi_m^* (-i\hbar \partial / \partial \varphi) \psi_m$ increases drastically as shown in Fig. 3, where L_z in each state is plotted as a function of R_{TF}/ξ_{dd} . The FL and CSV states both have a finite orbital angular momentum, but the dependence on R_{TF}/ξ_{dd} is quite different. Since the order parameters in the FL and CSV states are purely ferromagnetic, the spin texture depends only on R_{TF}/ξ_{dd} , and therefore L_z is independent of ξ_{sp} .

Finally, we discuss possible experimental situations. To form a spin texture in the ground state, the Zeeman energy must be smaller than the dipolar interaction energy; other-

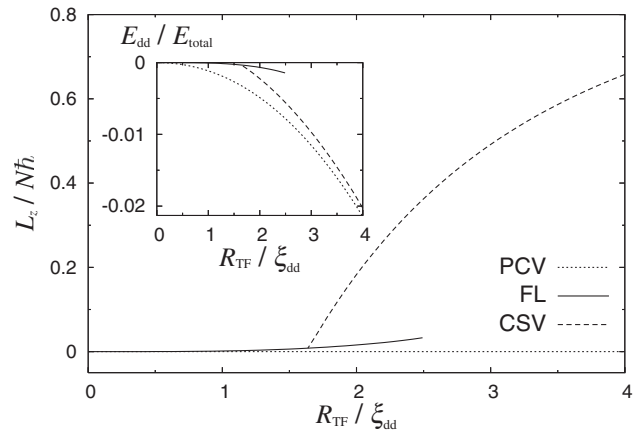


FIG. 3. Orbital angular momentum in each state as a function of R_{TF}/ξ_{dd} . The inset shows the ratio of the dipolar energy to the total energy $E_{dd}/E_{tot} \equiv \langle \hat{H}_{dd} \rangle / \langle \hat{H}_{tot} \rangle$ for each state at $R_{TF}/\xi_{sp} = 5.4$.

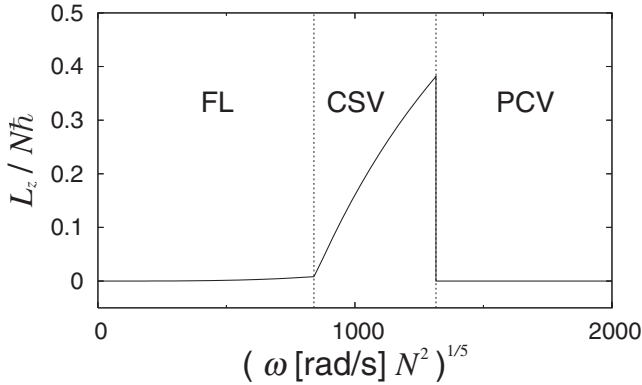


FIG. 4. Orbital angular momentum as a function of $(\omega N^2)^{1/5}$ for ^{87}Rb along the Rb line in Fig. 1.

wise the ground state is spin polarized. This implies that $B < 10^{-5}$ G for the spin-1 ^{87}Rb BEC with $n = 10^{15} \text{ cm}^{-3}$. The critical field increases in proportion to the atomic density. By changing the number of atoms or the trap frequency, all three phases we have found can be experimentally realized. Figure 4 shows the orbital angular momentum as a function of $(\omega N^2)^{1/5}$ along the Rb line in Fig. 1(a). In the case of a BEC with $N = 10^6$, for example, the CSV phase exists in the region of $2\pi \times 70 \text{ Hz} \leq \omega \leq 2\pi \times 630 \text{ Hz}$, where L_z increases up to $0.4N\hbar$. It is interesting to note that we can induce a phase transition by controlling the trap frequency.

In summary, we have investigated the phase diagram of a spin-1 ferromagnetic Bose-Einstein condensate with magnetic dipole-dipole interactions and found three phases, namely, the polar-core vortex phase, the flower phase, and the chiral spin-vortex phase. The chiral spin-vortex phase has chirality in the formation of the spin vortex, and the topological spin structure spontaneously yields a substantial net orbital angular momentum.

This work was supported by Grants in Aid for Scientific Research (Grant No. 17071005 and No. 17740263) and by 21st Century COE programs on “Nanometer-Scale

Quantum Physics” and “Coherent Optical Science” from the Ministry of Education, Culture, Sports, Science, and Technology of Japan. Y.K. acknowledges support by the Japan Society for Promotion of Science (Project No. 185451). M.U. acknowledges support by a CREST program of the JST.

Note added.—The ground-state phase diagram of a spinor dipolar system has recently been discussed in Ref. [13].

-
- [1] A. Hubert and R. Schäfer, *Magnetic Domains* (Springer-Verlag, Berlin, 1998).
 - [2] N.D. Mermin and T.-L. Ho, *Phys. Rev. Lett.* **36**, 594 (1976); T.-L. Ho and V.B. Shenoy, *Phys. Rev. Lett.* **77**, 2595 (1996).
 - [3] A. Griesmaier, J. Werner, S. Hensler, J. Stuhler, and T. Pfau, *Phys. Rev. Lett.* **94**, 160401 (2005); J. Stuhler, A. Griesmaier, T. Koch, M. Fattori, T. Pfau, S. Giovanazzi, P. Pedri, and L. Santos, *Phys. Rev. Lett.* **95**, 150406 (2005).
 - [4] S. Yi, L. You, and H. Pu, *Phys. Rev. Lett.* **93**, 040403 (2004).
 - [5] L. Santos and T. Pfau, *Phys. Rev. Lett.* **96**, 190404 (2006).
 - [6] R.B. Diener and T.-L. Ho, *Phys. Rev. Lett.* **96**, 190405 (2006).
 - [7] H. Pu, W. Zhang, and P. Meystre, *Phys. Rev. Lett.* **87**, 140405 (2001).
 - [8] K. Gross, C.P. Search, H. Pu, W. Zhang, and P. Meystre, *Phys. Rev. A* **66**, 033603 (2002).
 - [9] T.-L. Ho, *Phys. Rev. Lett.* **81**, 742 (1998); T. Ohmi and K. Machida, *J. Phys. Soc. Jpn.* **67**, 1822 (1998).
 - [10] T. Isoshima, K. Machida, and T. Ohmi, *J. Phys. Soc. Jpn.* **70**, 1604 (2001); T. Mizushima, N. Kobayashi, and K. Machida, *Phys. Rev. A* **70**, 043613 (2004).
 - [11] M.E. Schabes and N. Bertram, *J. Appl. Phys.* **64**, 1347 (1988).
 - [12] L. Landau and E. Lifshitz, *Phys. Z. Sowjetunion* **8**, 153 (1935).
 - [13] S. Yi and H. Pu, *Phys. Rev. Lett.* **97**, 020401 (2006).